Human Adipose-derived Mesenchymal Stem Cells-Derived Exosomes Encapsulated in Pluronic F127 Hydrogel Promote Wound Healing and Regeneration

Yang Zhou
Tongji University School of Medicine https://orcid.org/0000-0002-6967-421X
Xin-Liao Zhang
Tongji University School of Medicine
Hai-Jun Zhang
National United Engineering Laboratory for Biomedical Material Modification, Shandong, China
Yi-Jun Lu
Tongji University School of Medicine
Shou-Tao Lu
National United Engineering Laboratory for Biomedical Material Modification, Shandong, China
Bo Zhao
Tongji University School of Life Science and Thechology
Ning-Yan Zhang
Tongji University School of Life Science and Technology
Jing Zhang
Tongji University School of Life Science and Technology
Jun Zhang (junzhang@tongji.edu.cn)
Tongji University School of Medicine

Research Article

Keywords: wound healing, adipose-derived mesenchymal stem cells, exosomes, PF-127 hydrogel

Posted Date: July 2nd, 2021

DOI: https://doi.org/10.21203/rs.3.rs-670650/v1

Version of Record: A version of this preprint was published at Stem Cell Research & Therapy on August 8th, 2022. See the published version at https://doi.org/10.1186/s13287-022-02980-3.

Abstract

Background: Large area skin trauma has always been a great challenge for both patients and clinicians. Exosomes originated from human adipose-derived mesenchymal stem cells (hADSCs) have been a novel promising cell-free treatment in cutaneous damage repair. Nevertheless, the low retention rate of exosomes post-transplantation in vivo remains a significant challenge in clinical applications. Herein, we purposed to explore the potential clinical application roles of hADSCs-Exos encapsulated in functional PF-127 hydrogel in wound healing.

Methods: hADSCs-Exos were isolated from human hADSCs by ultracentrifugation. An injectable, biocompatible, and thermo-sensitive hydrogel Pluronic F-127 hydrogel was employed to encapsulate allogeneic hADSCs-Exos, and this complex was topically applied to a full-thickness cutaneous wound in mice. On different days post-transplantation, the mice were sacrificed, and the skin tissue was excised for histological and immunohistochemical analysis.

Results: PF-127/hADSCs-Exos complex enhanced skin wound healing, promoted re-epithelialization, increased expression of Ki67, α-SMA, and CD31, facilitated collagen synthesis (Collagen I, Collagen III), reduced inflammation (IL-6, TNF-α, CD68, CD206), and up-regulated expression of skin barrier proteins (KRT1, AQP3). The results showed that both PF-127/hADSCs-Exos and hADSCs-Exos could improve the cwound healing process at a similar level.

Conclusion: PF-127/hADSCs-Exos combination can maintain the bioactivity of hADSCs-Exos and control the exosome release. The low-frequency administration of PF-127/hADSCs-Exos could promote cutaneous wound healing instead of the high-frequency administration of pure exosomes. Thus, this biomaterial-based exosome will be a promising treatment approach for the cutaneous rejuvenation of skin wounds.

Introduction

The skin constitutes the human body's largest organ, accounting for about 8% of the total weight [1]. It covers the whole surface area and constitutes the first protective barrier to the external environment. So far, large-area skin trauma, burns, frostbite, and chronic wounds remain significant challenges for skin healing [2, 3]. The process of cutaneous wound healing is complex, initiated immediately after injury, and includes the multicellular overlapping and coordinated phases of inflammation, angiogenesis, and formation of granulation tissue, re-epithelialization, and fibroproliferation or matrix formation and remodeling [4, 5]. Unhealable wounds usually fail to follow the typical healing cascade, leading to stagnation in chronic inflammation and causing great pain to patients [6, 7].

The recent advancements in stem cell research have enabled stem cell-centered treatment to serve as a prospective alternative for rejuvenating wounds [8–12]. In particular, human adipose-derived mesenchymal stem cells (hADSCs) have exhibited highly remarkable ability for wound repair [13–15]. Recent research evidence has documented that exosome, 40–150 nm particles secreted by cells, can

regulate cell-to-cell communication via the transfer of the molecules they carrying, including mRNA, miRNAs, and proteins, to target cells [16]. Currently, it is recognized that MSC-Exos have a tissue-repair ability equal to or greater than that of MSCs themselves. Recent studies have also documented that MSC-Exos potentially enhance the wound healing process [17, 18]. Our previous study has illustrated that hADSCs-Exos can promote cell proliferation, angiogenesis, collagen synthesis, and skin barrier function repair, thereby accelerating cutaneous wound healing and revealing that hADSCs-Exos have a tissue-repair capacity more excellent than that of hADSCs themselves [19].

However, the utility of exosomes in treating wounds still faces some challenges since exosomes get cleared rapidly from the application site and survive in vivo for only a short time [20]. Therefore, the combination of exosomes with biomaterials that extend the retention time of exosomes on the wound surface without affecting their biological activity has become a focus of research to develop exosome-based therapies [21]. Tissue engineering-based strategy demonstrates that the utilization of biomaterial-based scaffolds as stem cell delivery and retention platforms can enhance the therapeutic efficiency of stem cells on wound regeneration [22].

Hydrogels have been regarded as promising biomaterials to deliver drugs/cells for wound therapeutics. Pluronic F-127, a synthetic and biocompatible hydrogel that has been approved for use in humans by FDA. It has been widely adopted as a scaffold for drug delivery, extracellular vesicles, as well as encapsulation of cells in tissue engineering [23]. Pluronic F-127, used as a wound-repair hydrogel scaffold, has some features, including injectable, biocompatible, and thermo-sensitive [24]. Recent reports also documented the adoption of hydrogels in delivering exosomes to restore vascularization and enhance wound regeneration [21]. However, the comprehensive assessment of the treatment effects and mechanism of combinations of hADSCs-Exos and F-127 for wound healing was very rare in reports.

In this study, we performed the topical administration of hADSCs-Exos in combination with PF-127. We explored whether topical application of hADSCs-Exos encapsulated in Pluronic F-127 hydrogel could accelerate the process of skin regeneration in cutaneous wound injury mice model. Our results showed that the hADSCs-Exos/ F-127 combination could better promote wound healing, cellular proliferation, enhance angiogenesis and collagen synthesis, and accelerate re-epithelialization by slowly releasing exosomes. Our results showed that the low-frequency administration of the hADSCs-Exos/F-127 combination could achieve the same therapeutic effect as topical application of hADSCs-Exos three times a day. It is suggested that the topical application of exosome-hydrogel combination is a simple and non-invasive treatment, potentially considered as a high-effective, low-toxicity delivery approach.

Methods And Materials

hADSCs culture and identification

hADSCs were obtained from the Stem Cell Bank of Shanghai East Hospital and were from three different random donors. hADSCs were processed, purified, and confirmed as previously described [19]. Concisely,

the hADSCs cells were cultured in a complete medium containing α-MEM (Gibco, USA) and 10% UltraGROTM-Advanced (Helios Bioscience, United States). Osteogenic, chondrogenic, and lipid induction were performed to characterize the hADSCs cell type.

hADSCs-Exos Extraction and Identification

After reaching 80–90% confluence, hADSCs were rinsed in dPBS and inoculated with freshly prepared complete medium for two days. After that, isolation of exosomes from the hADSCs culture medium by ultracentrifugation. The culture medium of hADSCs was centrifuged at 2000×g for 30 min at 4℃ to get rid of dead cells along with the debris, and then the supernate was transferred to a new 50 ml centrifuge tube, centrifuged at 10000×g for 30 min at 4℃ to get rid of other large vesicles. The supernatant would be collected again, put into a new 32ti rotor(Beckman Coulter, USA), centrifuged at 100000×g for 2 h 15min at 4℃. We removed the supernate, and re-suspended the pellets in dPBS, and kept them at − 80°C. The BCA protein assay kit was employed to determine protein quantitation of hADSCs exosomes (Thermo Fisher Scientific, United States). Conventional transmission electron microscopy coupled with NanoSight and Western blotting were adopted to explore hADSCs-Exos morphology, size, and marker expression (CD9, CD63, and CD81), respectively.

PF-127 hydrogel preparation and hADSCs-Exos encapsulation

PF-127 hydrogel preparation was performed according to the previous report [23, 24]. Briefly, 20%, 25% and 30% (w/v) Pluronic F-127 powder (Sigma, USA) was slowly dissolved in the precooled dPBS buffer solution by magnetic stirring at 4 ℃ overnight, then filtered with a 0.22 μm filter (Millipore, USA), and maintained at 4°C for use. hADSCs-Exos were encapsulated within PF-127 solution with 100ug, and the mixture was blended and stored at 4°C.

Release kinetics of PF-127 hydrogel encapsulated hADSCs-Exos

In vitro, to detect hADSCs-Exos released from the PF-127 hydrogel, we mixed hADSCs-Exos with 25% and 30% PF-127 at 4℃, then we put them in the transwell upper compartment placed in a 24-well plate at 37°C, and put 100 ul dPBS in the lower cells. We took the liquid from the lower chamber at 24h, 48h, 72h. We used the BCA approach to quantitate protein concentration in the lower chamber and calculate the amount percentage of released exosomes. In vivo experiment, the samples of PKH26-hADSCs-Exos encapsulated in the PF-127 hydrogel were topically administrated onto the wound. The concentration of released PKH26-exosomes was calculated by detecting the PKH26 fluorescence intensity in tissues at 24h, 48h, 72h, and 96h after treatment.

Wound healing experiments in an animal model

The 1.5 × 1.5 cm full-thickness wound of mice model was created as previously described [19]. All procedures were approved by the Animal Research Committee of Tongji University. Mice were randomized

into four groups: 1) Control group: no treatment; 2) PF-127 hydrogel group: 100 μl PF-127 hydrogel (25%); 3) hADSCs-Exos group: 100 μg hADSCs-Exos dissolved in 100 μl PBS; and 4) PF-127/hADSCs-Exos group: 100 μg hADSCs-Exos dissolved in 100 μl Pluronic F127 hydrogel (25%). The hADSCs-Exos were applied topically to the wound 3 times a day, while PF-127 hydrogel and PF-127/hADSCs-Exos group combination were performed once every three days. Post-operative mice were housed individually. The survival along with wound healing conditions for every group was documented.

Histological analysis, immunohistochemically and immunofluorescence staining

Wound samples were harvest after mice were sacrificed at days 1, 4, 7, 10, and 13 post-treatment. The worst part of each wound healing condition was selected for analysis. Tissue sections (5μm) were mounted on slides for histological analysis. H&E and Masson's trichrome staining were adopted to visualize the pathological changes in the rejuvenated tissue and collagen formation at the varied healing time.

For immunohistochemically (IHC) and immunofluorescence (IF) staining, the dewaxed sections were washed in PBS, and the endogenous peroxidase activity was quenched by immersion in 2%(v/v) hydrogen peroxide for 5 minutes. The antigen retrieval was repaired by incubation with sodium citrate buffer for 30 minutes. After rinsing in PBS, the sections were sealed with 1.5% goat serum at room temperature for 30 minutes and then incubated with primary antibodies anti-Ki67 (Abcam, Cambridge, MA), anti-α-SMA (Abcam, MA), anti-CD31 (Abcam, MA), anti-Collagen I (Abcam, MA), anti- Collagen III (Abcam, MA), anti-IL-6 (Boster Biological Technology, China), anti-TNF-α (Boster Biological Technology, China), anti-CD68 (Boster Biological Technology, China), anti-CD206 (Boster Biological Technology, China), anti-Keratin1 (KRT1) (Abcam, MA), anti-AQP3 (Abcam, MA) overnight at 4℃, and then inoculated with corresponding secondary antibody (goat anti-rabbit or goat anti-mouse, ZSGB-BIO). Images were acquired using a BX53 microscope (Olympus, Japan) and analyzed with Image-Pro Plus 6.0 software. Six animals per group were analyzed for IHC staining. For each sample, we randomly selected at least five fields for analysis.

Western blotting

Protein concentration Total protein in exosomes was extracted by RIPA and quantified using the BCA protein assay kit (Pierce). Fractionation of proteins was done on the 10% SDS-PAGE gels and was transfer-embedded onto Hybond-P polyvinylidene difluoride (PVDF) membrane (Millipore). Afterward, membranes were blocked and then was inoculated overnight with the antibodies at 4°C. Subsequently, the membranes were rinsed in 1 × TBST and then incubated with a secondary antibody in a 37°C incubator for two hours. Protein bands were analyzed using Amersham Imager 600 system (GE). The antibodies (all from Abcam, Cambridge, MA) used consisted of anti-CD81 (1:1000), anti-CD9 (1:1000), anti-Tubllin (1:1000), and anti-CD63 (1:1000).

Statistical analysis

Statistical analysis was performed using GraphPad Prism software. In the case of more than two groups of samples, one-way ANOVA was used with one condition, and two-way ANOVA was used with more than two conditions. ANOVA analysis was followed by post hoc Bonferroni's correction for multiple comparisons. $p < 0.05$ was taken as statistically significant; *p-value < 0.05, **p-value < 0.01, ***p-value < 0.001, ****p-value < 0.0001. Data from at least three individual experiments are listed as mean ± standard deviation (mean ± SD) or mean ± standard Error of Mean(mean ± SEM).

Result

hADSCs-Exos isolation and characterization

As illustrated in Fig. 1a, the obtained hADSCs cells displayed classical fibroblast-like morphology along with a plastic-adherent property. These cells showed the ability to differentiate into osteoblasts, adipocytes, and chondrocytes (Fig. 1b). Flow cytometry data demonstrated that hADSCs were remarkably positive for MSC surface biomarkers CD73, CD90, and CD105, however negative for CD45 and HLA-DR (Fig. 1c), which are consistent with the results reported in previous studies. The hADSCs-Exos were harvested from the serum-free medium of hADSCs by ultracentrifugation (Fig. 1d). TEM data exhibited that hADSCs-Exos were saucer-like structurally (Fig. 1e), with diameters of between 30 and 100 nm. Nanosight analysis was adopted to assess the diameter size distribution and the particle concentration of hADSCs-Exos (Fig. 1f). Western blot results showed that hADSCs-Exos expressed exosome surface markers, including CD9, CD63, CD81 (Fig. 1g). All these data illustrated that hADSCs-Exos were successfully isolated in this study.

Exosome-Hydrogel Complexes Temperature Sensitivity and Release Profile

This study tested the gelling time of 20%, 25%, and 30% (w/v) Pluronic F-127 with 100ug hADSCs-Exos at 35℃, 36℃, and 37℃, respectively (Table 1). As the Pluronic F-127 concentration increased, the gelling time of PF-127/hADSCs-Exos decreased. The 20% PF-127/hADSCs-Exos composite gelled at 37°C with 17s, while the 30% PF-127/hADSCs-Exos composite gelled at 2.7s at the same temperature. In addition, the gel formation time was inversely proportional to the temperature. The prepared 20% PF-127/hADSCs-Exos mixture was liquid at 4°C and in a gelation status at 37°C. The above results revealed that it took more time for 20% PF-127/hADSCs-Exos composite to form gel than the 25% and 30% PF-127/hADSCs-Exos mixtures.

Table 1
Gelling Time of Gel Complex in Different PF-127 Concentration and on Different Temperature (Mean ± sd)

PF-127 Concentration	Gelling Time at 35°C	Gelling Time at 36°C	Gelling Time at 37°C
20%	20.3 ± 1.5	18 ± 1	17 ± 0.5
25%	5.7 ± 1.2	4.7 ± 0.6	3.7 ± 0.6
30%	3.7 ± 0.6	3.3 ± 0.6	2.7 ± 0.6

Then, 25% and 30% PF-127/hADSCs-Exos mixtures were chosen to detect the release ability of the hADSCs-Exos. In vitro, the hADSCs-Exos encapsulated in the PF-127 hydrogel could be released steadily over a long time. Compared with the 30% PF-127, 25% PF-127 hydrogel could provide a stable and effective platform for hADSCs-Exos encapsulation and sustained release (Fig. 2a, b). To detect the sustained release of hADSCs-Exos in vivo, hADSCs-Exos were labeled with PKH26 and encapsulated in the 25% PF-127 hydrogel. When PKH26-hADSCs-Exos were applied alone on the wound, the fluorescence signal of exosomes became undetectable 96 hours after transplantation, but PKH26-hADSCs-Exos encapsulated in the 25% PF-127 hydrogel can still be detected after 96 hours (Fig. 2c). All these data indicated that 25% PF-127 hydrogel could maintain the sustained release of hADSCs-Exos and ensure the effective time of hADSCs-Exos for skin wound healing.

PF-127/hADSCs-Exos promotes cutaneous wound healing in mice

Full-thickness skin wounds on the backs of mice were created and treated with PF-127/hADSCs-Exos, hADSCs-Exos, PF-127 hydrogel, or no treatment. Representative images of wound area in each group at 1, 4, 7, 10, and 13 days after surgery are illustrated (Fig. 3a). On days 1, 4, 7, and 10 days after transplantation, the wound-healing rate in the PF-127/hADSCs-Exos composite treatment group was remarkably higher in contrast with that in other groups (Fig. 3b). The histologic structures of the regenerated dermis were analyzed on days 1, 4, 7, 10, and 13. As illustrated in Fig. 3c, the epidermis of the new granulation tissue is integrated, as well as thick in both PF-127/hADSCs-Exos and hADSCs-Exos groups. However, in the PF-127/hADSCs-Exos group, generation of new hair follicles was evident at the wound center, proliferating fibroblasts were detected under the epidermis, with orderly and sufficient collagen deposition observed, which were not seen in the hADSCs-Exos alone group. For PF-127 alone and the control groups, there was no evidence of integration in the epidermal structure, with only a thin dermal layer observed. In addition, apparent inflammatory cell in filtration was still observed on day 13. Furthermore, we observed narrower scar areas in wounds under the hADSCs-Exos and PF-127/hADSCs-Exos treatment in contrast with the control wounds (Fig. 3d, e). All these data demonstrated that the PF-127 hydrogel supported hADSCs-Exos survival and biological activity and accelerated the healing process of the wound in mice.

PF-127/hADSCs-Exos improve cell proliferation and angiogenesis

To explore the potential therapeutic mechanism of how the topical application of hADSCs-Exos, PF-127 hydrogel, and hADSCs-Exos laden on PF-127 hydrogel affects the cells in the granulation tissues, we performed the IHC analysis of Ki67, CD31, and α-SMA. Ki67 was performed to determine total cellular proliferation. As shown in Fig. 4a and b, the number of Ki67 positive cells in the PF-127/hADSCs-Exos combination group and hADSCs-Exos group significantly increased compared to other groups. Following the PF-127/hADSCs-Exos combination and hADSCs-Exos treatment, the higher expression levels of the myofibroblast marker α-SMA were detected compared to in other groups (Fig. 4c and d). Then, the levels CD31 were measured to assess newly formed vessels in the regenerated tissue. The endothelial cell marker CD31 was also used to confirm tissue vascularization. Figures 4e and f showed that PF-127/hADSCs-Exos and the hADSCs-Exos group had remarkable blood vessel numbers in contrast with the PF-127 alone and the control groups after seven days of treatment.

PF-127/hADSCs-Exos can promote collagen synthesis, skin barrier repair

Proper collagen deposition and remodeling could enhance the tissue tensile strength and lead to a better healing effect. There was remarkably more deposition of newly formed collagen in wounds under PF-127/hADSCs-Exos treatment than others at days 4, 7, 10, and 13 (Fig. 5a and b). Collagen I and III are the main ECM components in the dermis, and their formation has an indispensable role in wound healing. Thus, immunostaining was employed to explore the collagen□/□ contents in the wound tissues. As shown in Fig. 5c - f, the deposition amount of collagen□and □ depicted similar changing patterns to Masson staining. With the increase in healing time, the deposition of collagen I and III increased in all wounds. At the same time, the PF-127/hADSCs-Exos and the hADSCs-Exos group showed significantly higher intensity and a lower anti-scarring ratio of collagen I to collagen III than other groups (Fig. 5g). It is known that scarless healing fetal wounds accumulate more collagen type III in contrast with scarring adult wounds, which have a higher percentage of type I collagen deposition [27–29]. These data indicated that PF-127/hADSCs-Exos could accelerate the collagen deposition of the wound site, decrease the scar formation, and improve the healing quality of wound tissue, with the same effect as hADSCs-Exos.

The stratum corneum is the outer layer of the epithelium, which is responsible for the skin barrier permeability and the cornified epithelium resilience. As a remarkable cellular cytoskeleton constituent, keratins constitute the largest subgroup of intermediate filament proteins. KRT1, a keratin family member of cytoskeleton proteins, primarily expressed in skin epithelium. On the 13th day, PF-127/hADSCs-Exos and hADSCs-Exos treated wounds exhibited lower expression of KRT1 than other groups (Fig. 6a and b). AQP3 is the dominant aquaporin in human skin, located in the basal layer of the epidermis and the stratum corneum, playing a central role in skin hydration. As illustrated in Fig. 6c and d, on the 13days, the expression of AQP3 in the PF-127/hADSCs-Exos treatment group was remarkably higher than that in other groups, followed by pure exosomes treated wounds. These data showed that PF-127/hADSCs-Exos

improves skin hydration, the elasticity of the skin after trauma, and epidermal permeability barrier function.

PF-127/hADSCs-Exos can decrease inflammation

Inflammation constitutes the initial response of the phrases of the typical wounding repair. To explore the influence of PF-127/hADSCs-Exos hydrogel treatment on inflammation, the expression level of cytokines, and chemokines, like tumor necrosis factor (TNF) - α and interleukin (IL)-6 were analyzed with IHC. The results showed that PF-127/hADSCs-Exos could alleviate the inflammatory response by downregulating TNF-α and IL-6 (Fig. 7a – d). Besides, macrophages persist across all the stages of the repair process of skin wound healing. M1-like macrophages are expressed in the early inflammatory phase and promote the inflammatory reaction. M2-like macrophages can dampen inflammation and initiate tissue repair through releasing anti-inflammatory cytokines and promote tissue repair [30]. We employed immunohistochemistry technology to explore the expression of CD68 (a pan marker for all macrophages) and CD206 (a marker for M2-like macrophages) [31]. The results showed that PF-127/hADSCs-Exos and hADSCs-Exos could decrease the expression level of CD68 and increase the level of CD206 (Fig. 7e – h). All these results indicated that PF-127/hADSCs-Exos and hADSCs-Exos could reduce wound inflammation by down-regulating the expression TNF-α, IL-6, CD68, and up-regulated CD206 expression.

Discussion

In this study, we constructed a PF-127/hADSCs-Exos combination and applied it to a mouse cutaneous injury model to validate its capacity to prolong exosome survival in vitro efficiently. The PF-127/hADSCs-Exos composite can significantly promote skin wound healing and maintain the bioactivity of hADSCs-Exos. Our study revealed that PF-127/hADSCs-Exos treatment once three days can achieve the same therapeutic effect as an hADSCs-Exos treatment three times a day.

hADSCs are regarded as a promising cell arsenal for stem cell treatments and tissue regeneration due to their beneficial features, e.g., easy isolation, self-renewal potential, multi-potency, as well as immune-modulatory effects [32, 33]. hADSCs have been illustrated to accelerate wound healing by promoting neo-angiogenesis, collagen synthesis, and reduce inflammation [34, 35]. Our previous studies have shown that topical administration of hADSCs-Exos is more beneficial for promoting skin damage repair than hADSCs themselves [19]. However, the rapid clearance and low survival rate are significant challenges for the topical application of hADSCs-Exos on the wound. The therapeutic efficacy of hADSCs-Exos for wound healing needs to be further improved.

Tissue engineering and regenerative medicine have recently mushroomed as a hotspot approach of facilitating the rejuvenation of wounded tissue [22, 36]. These bioengineering technologies that entail utilizing biomaterial, stem cells, and biologically active factors, have been widely studied in skin soft tissue defects [37]. Numerous reports have documented that Pluronic F-127 is a prospective scaffold for encapsulating MSCs or exosomes to promote the regeneration of poorly vascularized tissues, such as epithelial, cartilage, tendons, or even bony and adipose tissues [23]. Hydrogel has unique properties,

including thermosensitivity, enabling it to easily encapsulate cells and allowing high cell numbers to adhere at the wound site [38]. Considering that the initial gelation temperature of PF-127 hydrogel reduces with escalating concentration, 25% PF-127 exhibited an average gel time and was thus chosen as the exosome carrier according to our results.

The functionality of exosomes primarily depends on their molecular components consisting of DNA, RNA, and proteins. Nonetheless, MSC-originated exosomes have short residence time due to their rapid clearance in vivo [20]. In order to attain a sustained treatment effect, multiple smearing of exosomes is required for topical wound treatment, which is not appropriate for patients. Therefore, increasing the time of retention by using biomaterials to deliver exosomes represents a better strategy. Our results demonstrated that the Pluronic F-127 hydrogel could be utilized to ensure a sustained, as well as steady release of hADSCs-Exos in vitro (Fig. 2a) and in vivo (Fig. 2b).

Wound healing is a delicate and complicated process, and large area skin trauma has always been a great challenge for both patients and clinicians. Skin wound regeneration is complex, and it entails blood coagulation, inflammation, new tissue formation, and tissue remodeling [2]. Diminished proinflammatory cytokines, compromised neovascularization, and impairment in leukocyte mobilization might disturb and delay wound healing. In this study, we topically applied hADSCs-Exos to the wound sites three times a day and PF-127/hADSCs-Exos once three days. PF-127/hADSCs-Exos group and hADSCs-Exos group exhibited faster healing rates in contrast with those of other groups during the whole healing process, which showed that PF-127/hADSCs-Exos complex could protect the biological activity of hADSCs-Exos, and release these exosomes continuously, resulting in increased, sustained, as well as rapid wound healing.

To explore the mechanisms of treatment impacts on wound healing at injury sites, we performed the IHC staining of a cellular marker Ki67 to investigate potential mechanisms how the topical administration of PF-127/hADSCs-Exos, hADSCs-Exos, and PF-127 affects the cells proliferation in the wound tissues. As shown in Fig. 4a and b, more active host cell proliferation (positive Ki67 cells) was observed in the PF-127/hADSCs-Exos and hADSCs-Exos group wounds than that in the other groups. Furthermore, the expression levels of myofibroblast marker α-SMA were increased, indicating that both PF-127/hADSCs-Exos and hADSCs-Exos could promote the myofibroblasts formation effectively. The IHC staining of endothelial marker CD31 and indicated that hADSCs-Exos enhanced angiogenesis in PF-127/hADSCs-Exos and hADSCs-Exos-treated compared with PF-127 alone and control groups. Both PF-127/hADSCs-Exos and hADSCs-Exos could promote cell proliferation and angiogenesis and facilitate the synthesis of granulation tissue at the wound site. Thus, PF-127/hADSCs-Exos can achieve the same therapeutic effect as topical application of hADSCs-Exos.

The type □ and □ collagen is the main component of dermal ECM, which plays an essential role in wound healing. PF-127/hADSCs-Exos and hADSCs-Exos significantly increased the deposition of collagen-I and collagen-III. It has been reported that abundant deposition of collagen-III in the early stage of the would facilitate healing and result in scarless skin [28, 39, 40]. hADSCs-Exos could promote ECM reconstruction

in cutaneous wounds healing by modulating the ratios of collagen type III to type I with regulating differentiation of fibroblast to suppress scar formation [39]. With the increase in healing time, the ratios of collagen I to collagen III were decreased c PF-127/hADSCs-Exos and hADSCs-Exos-treated groups, promoting to form of scar-free wounds.

Meanwhile, PF-127/hADSCs-Exos and hADSCs-Exos regulated the expression levels of KRT1 and AQP3. KRT1 can maintain skin integrity and participates in an inflammatory network in the skin, and its expression level correlates with the degree of inflammation [41]. The elevated AQP3 expression might lead to an increased moisture content of dermal tissues, enhanced skin texture, increased skin elasticity, and the potential to repair wounds and other injuries [42]. In our study, KRT1, a lower expression level of KRT1 was observed in PF-127/hADSCs-Exos and hADSCs-Exos -treated groups, while a higher expression level of AQP3 was detected. It revealed that PF-127/hADSCs-Exos could promote the re-epithelialization with the same as pure hADSCs-Exos.

The four phases of the classical wound repair process begin with inflammation. We found that PF-127/hADSCs-Exos and hADSCs-Exos can alleviate the inflammatory response by downregulating TNF-α, IL-6, inhibiting M1 macrophage formation, and promoting M2 macrophages formation. These data revealed that the use of the PF-127/hADSCs-Exos complex could maintain the survival of hADSCs-Exos in the inflammatory environment of a wound and retain hADSCs-Exos vitality. Their numbers increase in the inflammation phase, attaining the peak at the granulation tissue formation; however, the decline in the final phase of maturation. In our study, the cells with $CD68^{+}$, a pan marker for macrophage, were markedly decreased in the PF-127/hADSCs-Exos and hADSCs-Exos treatment groups, suggested that the mild inflammatory reactions occurred in the wound area after PF-127/hADSCs-Exos and hADSCs-Exos treated. In addition, the phenotype of macrophages in the wound is influenced by the wound microenvironment and can be roughly divided into two groups: M1 and M2 macrophages [30]. M2-like macrophages possess pro-tissue repair, as well as anti-inflammatory characteristics. They possess the mannose receptor CD206 [43]. The numbers of $CD206^{+}$ M2-like macrophages were increased in the PF-127/hADSCs-Exos and hADSCs-Exos treatment groups, suggested that PF-127/hADSCs-Exos and hADSCs-Exos can reduce the inflammatory reaction by promoting the M2-like macrophages formation.

All these above results indicated that more significant numbers of functional hADSCs-Exos were potentially maintained and released continually during PF-127 hydrogel-based delivery to the skin wound, which ultimately contributes to its effectiveness in full-thickness cutaneous wound healing. Nevertheless, the mechanism of wound repair induced by hADSCs-Exos is still unclear, and specific signaling pathways need to be explored in future work.

Conclusion

In the current study, we successfully applied allogeneic hADSCs-Exos encapsulated in a PF-127 thermosensitive hydrogel for treating wounds. The PF-127/hADSCs-Exos complexes maintained the biological activity of hADSCs-Exos and enhanced cell proliferation, angiogenesis, collagen remodeling,

and re-epithelialization at the wound sites, and accelerated the wound healing process. PF-127/hADSCs-Exos treatment once three days can achieve the same therapeutic effect as an hADSCs-Exos treatment three times a day. The results provide sufficient research evidence for treating wounds with PF-127/hADSCs-Exos complexes. PF-127 thermosensitive hydrogel as a delivery scaffold is suitable for delivering and continuously releasing hADSCs-Exos on the wound site. Our study revealed that topically transplanted PF-127/hADSCs-Exos complexes are promising novel treatment alternatives for wound healing.

Abbreviations

hADSCs: human adipose-derived mesenchymal stem cells; hADSCs-Exos: human adipose-derived mesenchymal stem cells derived exosomes; TEM: Transmission electron microscopy; NTA: Nanosight tracking analysis; PBS: Phosphate-buffered saline; SEM: Scanning electron microscopy

Declarations

Acknowledgements

We thank the Translational Medical Center for Stem Cell Therapy of Shanghai East Hospital for their assistance and guidance for hADSCs culture.

Funding

This research project was supported by the National Natural Science Foundation of China (81771417, 31371379 and 31271120), the National Key Research and Development Program of China [2016YFA0700800], Major Program of Development Fund for Shanghai Zhangjiang National Innovation Demonstration Zone <Stem Cell Strategic Biobank and Stem Cell Clinical Technology Transformation Platform> [ZJ2018-ZD-004], the Peak Disciplines (Type IV) of Institutions of Higher Learning in Shanghai.

Availability of data and materials

Data and reagents will be provided upon availability and reasonable request.

Authors' contributions

YZ conceived the idea for the project, designed all experiments, and analyzed data. XLZ performed major experiments and analyzed data. HJZ, YJL, STL, BZ, and NYZ assisted in performing experiments. YZ and XLZ wrote the manuscript. JZ and JZ verified the final version of the manuscript. All authors read and approved the final manuscript.

Ethics approval and consent to participate

All human samples and animal studies were approved by the Committee of Ethics on Experimentation of Tongji University. The experiments were conducted in accordance with the National Institutes of Health guidelines for the care and use of animals.

Consent for publication

Not applicable.

Competing interests

The authors declare that they have no competing interests.

References

1. Wang P. H., Huang B. S., Horng H. C., Yeh C. C., Chen Y. J. Wound healing, Journal of the Chinese Medical Association : JCMA 2018: 81: 94-101.
2. Bhardwaj N., Chouhan D., Mandal B. B. Tissue Engineered Skin and Wound Healing: Current Strategies and Future Directions, Current pharmaceutical design 2017: 23: 3455-3482.
3. Takeo M., Lee W., Ito M. Wound healing and skin regeneration, Cold Spring Harbor perspectives in medicine 2015: 5: a023267.
4. Jeschke M. G., Patsouris D., Stanojcic M., Abdullahi A., Rehou S., Pinto R. et al. Pathophysiologic Response to Burns in the Elderly, EBioMedicine 2015: 2: 1536-1548.
5. Han G., Ceilley R. Chronic Wound Healing: A Review of Current Management and Treatments, Advances in therapy 2017: 34: 599-610.
6. Kim H., Wang S. Y., Kwak G., Yang Y., Kwon I. C., Kim S. H. Exosome-Guided Phenotypic Switch of M1 to M2 Macrophages for Cutaneous Wound Healing, Adv Sci (Weinh) 2019: 6: 1900513.
7. Mead B., Ahmed Z., Tomarev S. Mesenchymal Stem Cell-Derived Small Extracellular Vesicles Promote Neuroprotection in a Genetic DBA/2J Mouse Model of Glaucoma, Investigative ophthalmology & visual science 2018: 59: 5473-5480.
8. Lei Z., Singh G., Min Z., Shixuan C., Xu K., Pengcheng X. et al. Bone marrow-derived mesenchymal stem cells laden novel thermo-sensitive hydrogel for the management of severe skin wound healing, Materials science & engineering C, Materials for biological applications 2018: 90: 159-167.
9. Phinney D. G., Pittenger M. F. Concise Review: MSC-Derived Exosomes for Cell-Free Therapy, Stem cells (Dayton, Ohio) 2017: 35: 851-858.
10. Mead B., Tomarev S. Bone Marrow-Derived Mesenchymal Stem Cells-Derived Exosomes Promote Survival of Retinal Ganglion Cells Through miRNA-Dependent Mechanisms, Stem cells translational medicine 2017: 6: 1273-1285.
11. Li P., Guo X. A review: therapeutic potential of adipose-derived stem cells in cutaneous wound healing and regeneration, Stem cell research & therapy 2018: 9: 302.

12. Kanji S., Das H. Advances of Stem Cell Therapeutics in Cutaneous Wound Healing and Regeneration, Mediators of inflammation 2017: 2017: 5217967.
13. Holm J. S., Toyserkani N. M., Sorensen J. A. Adipose-derived stem cells for treatment of chronic ulcers: current status, Stem cell research & therapy 2018: 9: 142.
14. Franck C. L., Senegaglia A. C., Leite L. M. B., de Moura S. A. B., Francisco N. F., Ribas Filho J. M. Influence of Adipose Tissue-Derived Stem Cells on the Burn Wound Healing Process, Stem Cells Int 2019: 2019: 2340725.
15. Tyeb S., Shiekh P. A., Verma V., Kumar A. Adipose-Derived Stem Cells (ADSCs) Loaded Gelatin-Sericin-Laminin Cryogels for Tissue Regeneration in Diabetic Wounds, Biomacromolecules 2020: 21: 294-304.
16. Hessvik N. P., Llorente A. Current knowledge on exosome biogenesis and release, Cell Mol Life Sci 2018: 75: 193-208.
17. Zhang W., Bai X., Zhao B., Li Y., Zhang Y., Li Z. et al. Cell-free therapy based on adipose tissue stem cell-derived exosomes promotes wound healing via the PI3K/Akt signaling pathway, Experimental cell research 2018: 370: 333-342.
18. Qiu H., Liu S., Wu K., Zhao R., Cao L., Wang H. Prospective application of exosomes derived from adipose-derived stem cells in skin wound healing: A review, J Cosmet Dermatol 2020: 19: 574-581.
19. Zhou Y., Zhao B., Zhang X. L., Lu Y. J., Lu S. T., Cheng J. et al. Combined topical and systemic administration with human adipose-derived mesenchymal stem cells (hADSC) and hADSC-derived exosomes markedly promoted cutaneous wound healing and regeneration, Stem cell research & therapy 2021: 12: 257.
20. Liu X., Yang Y., Li Y., Niu X., Zhao B., Wang Y. et al. Integration of stem cell-derived exosomes with in situ hydrogel glue as a promising tissue patch for articular cartilage regeneration, Nanoscale 2017: 9: 4430-4438.
21. Yang J., Chen Z., Pan D., Li H., Shen J. Umbilical Cord-Derived Mesenchymal Stem Cell-Derived Exosomes Combined Pluronic F127 Hydrogel Promote Chronic Diabetic Wound Healing and Complete Skin Regeneration, Int J Nanomedicine 2020: 15: 5911-5926.
22. Mao A. S., Mooney D. J. Regenerative medicine: Current therapies and future directions, Proc Natl Acad Sci U S A 2015: 112: 14452-14459.
23. Diniz I. M., Chen C., Xu X., Ansari S., Zadeh H. H., Marques M. M. et al. Pluronic F-127 hydrogel as a promising scaffold for encapsulation of dental-derived mesenchymal stem cells, Journal of materials science Materials in medicine 2015: 26: 153.
24. Dung T. H., Huong L. T., Yoo H. Morphological Feature of Pluronic F127 and Its Application in Burn Treatment, Journal of nanoscience and nanotechnology 2018: 18: 829-832.
25. Zhu Z., Hou Q., Li M., Fu X. Molecular mechanism of myofibroblast formation and strategies for clinical drugs treatments in hypertrophic scars, J Cell Physiol 2020: 235: 4109-4119.
26. Nakagami H., Sugimoto K., Ishikawa T., Fujimoto T., Yamaoka T., Hayashi M. et al. Physician-initiated clinical study of limb ulcers treated with a functional peptide, SR-0379: from discovery to a

randomized, double-blind, placebo-controlled trial, NPJ aging and mechanisms of disease 2018: 4: 2.

27. Zhang J., Guan J., Niu X., Hu G., Guo S., Li Q. et al. Exosomes released from human induced pluripotent stem cells-derived MSCs facilitate cutaneous wound healing by promoting collagen synthesis and angiogenesis, J Transl Med 2015: 13: 49.
28. Wang T., Gu Q., Zhao J., Mei J., Shao M., Pan Y. et al. Calcium alginate enhances wound healing by up-regulating the ratio of collagen types I/III in diabetic rats, Int J Clin Exp Pathol 2015: 8: 6636-6645.
29. Volk S. W., Wang Y., Mauldin E. A., Liechty K. W., Adams S. L. Diminished type III collagen promotes myofibroblast differentiation and increases scar deposition in cutaneous wound healing, Cells Tissues Organs 2011: 194: 25-37.
30. Klar A. S., Michalak-Micka K., Biedermann T., Simmen-Meuli C., Reichmann E., Meuli M. Characterization of M1 and M2 polarization of macrophages in vascularized human dermo-epidermal skin substitutes in vivo, Pediatr Surg Int 2018: 34: 129-135.
31. Ren C. X., Leng R. X., Fan Y. G., Pan H. F., Li B. Z., Wu C. H. et al. Intratumoral and peritumoral expression of CD68 and CD206 in hepatocellular carcinoma and their prognostic value, Oncol Rep 2017: 38: 886-898.
32. Mastrolia I., Foppiani E. M., Murgia A., Candini O., Samarelli A. V., Grisendi G. et al. Challenges in Clinical Development of Mesenchymal Stromal/Stem Cells: Concise Review, Stem cells translational medicine 2019: 8: 1135-1148.
33. Kokai L. E., Marra K., Rubin J. P. Adipose stem cells: biology and clinical applications for tissue repair and regeneration, Transl Res 2014: 163: 399-408.
34. Ahmadi A. R., Chicco M., Huang J., Qi L., Burdick J., Williams G. M. et al. Stem cells in burn wound healing: A systematic review of the literature, Burns 2019: 45: 1014-1023.
35. Goodarzi P., Alavi-Moghadam S., Sarvari M., Tayanloo Beik A., Falahzadeh K., Aghayan H. et al. Adipose Tissue-Derived Stromal Cells for Wound Healing, Adv Exp Med Biol 2018: 1119: 133-149.
36. Deng Q., Huang S., Wen J., Jiao Y., Su X., Shi G. et al. PF-127 hydrogel plus sodium ascorbyl phosphate improves Wharton's jelly mesenchymal stem cell-mediated skin wound healing in mice, Stem cell research & therapy 2020: 11: 143.
37. Gentile P., Scioli M. G., Bielli A., Orlandi A., Cervelli V. Concise Review: The Use of Adipose-Derived Stromal Vascular Fraction Cells and Platelet Rich Plasma in Regenerative Plastic Surgery, Stem cells (Dayton, Ohio) 2017: 35: 117-134.
38. Kaisang L., Siyu W., Lijun F., Daoyan P., Xian C. J., Jie S. Adipose-derived stem cells seeded in Pluronic F-127 hydrogel promotes diabetic wound healing, J Surg Res 2017: 217: 63-74.
39. Wang L., Hu L., Zhou X., Xiong Z., Zhang C., Shehada H. M. A. et al. Exosomes secreted by human adipose mesenchymal stem cells promote scarless cutaneous repair by regulating extracellular matrix remodelling, Sci Rep 2017: 7: 13321.
40. Monavarian M., Kader S., Moeinzadeh S., Jabbari E. Regenerative Scar-Free Skin Wound Healing, Tissue Eng Part B Rev 2019: 25: 294-311.

41. Roth W., Kumar V., Beer H. D., Richter M., Wohlenberg C., Reuter U. et al. Keratin 1 maintains skin integrity and participates in an inflammatory network in skin through interleukin-18, J Cell Sci 2012: 125: 5269-5279.
42. Maharlooei M. K., Bagheri M., Solhjou Z., Jahromi B. M., Akrami M., Rohani L. et al. Adipose tissue derived mesenchymal stem cell (AD-MSC) promotes skin wound healing in diabetic rats, Diabetes Res Clin Pract 2011: 93: 228-234.
43. Wang J., Xu L., Xiang Z., Ren Y., Zheng X., Zhao Q. et al. Microcystin-LR ameliorates pulmonary fibrosis via modulating CD206(+) M2-like macrophage polarization, Cell Death Dis 2020: 11: 136.

Figures

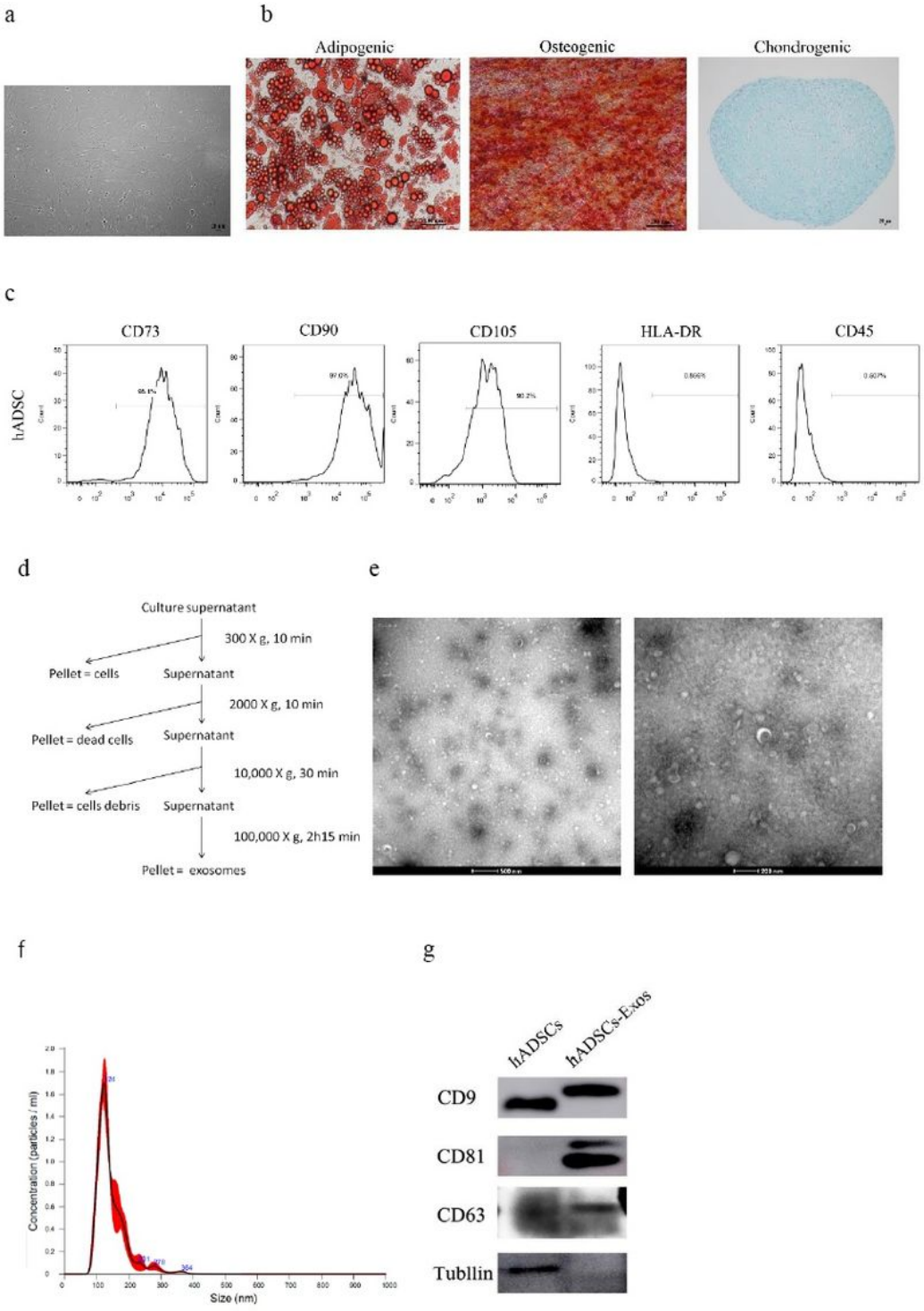

Figure 1

Characterization of hADSCs and hADSCs-Exos. a Microscopic images of hADSCs. Scale bar = 20 μm. b hADSCs differentiated into adipocytes – Oil Red O (red), osteoblasts – RunX2 (red), and chondrocytes – alcian blue (blue). c Detection of the specific markers of hADSCs by flow cytometry illustrated that hADSCs were positive for CD90, CD73, and CD105, negative for HLA-DR, and CD45. d hADSCs- Exos

Ultracentrifugation extraction. hADSCs-Exos were identified by electron microscope (e), NanoSight (f), and Western blot (g).

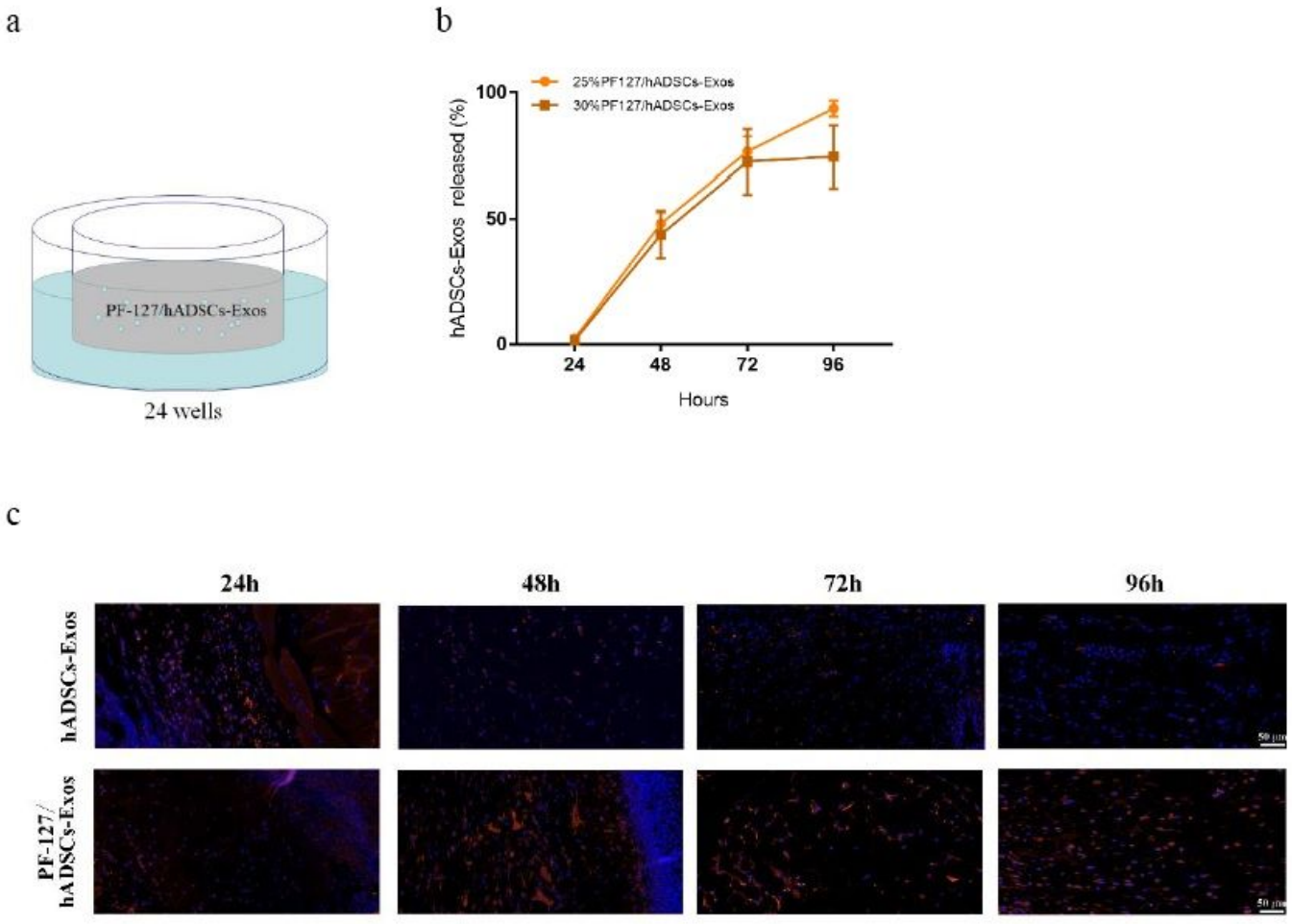

Figure 2

PF-127/hADSCs-Exos complexes allow the stable release of hADSCs-Exos. a Schematic representation of the experimental approach. b The cumulative release ratio of hADSCs-Exos was detected by protein quantification. c hADSCs-Exos retention in the site of the wound. Scale bar = 50 μm.

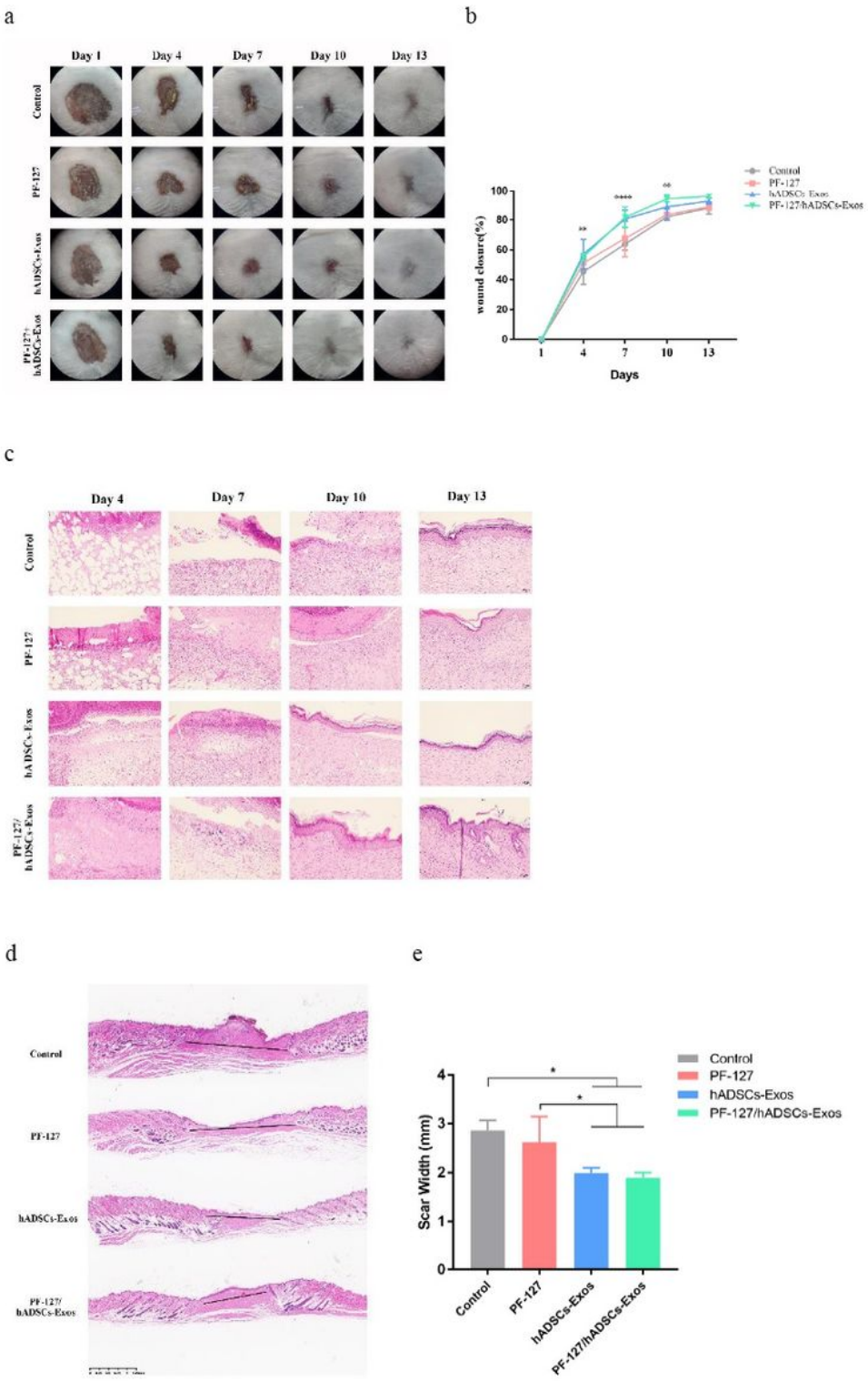

Figure 3

PF-127/hADSCs-Exos complexes promote cutaneous wound healing. a Representative images of the skin wound healing in each group on days 1, 4, 7, 10, and 13. b Quantitation data of the ratio of the wound healing in each group. The wound closure rate was computed using the Wound healing rate = (W0-Wd)/W0×100%. W0 wound area on day 0. Wd wound area on day d post-treatment. c Wounded skin

sections stained with H&E in diverse groups at day 4, 7, 10, and 13 post-wounding. Scale bar = 20 μm. *p-value < 0.05, **p-value < 0.01, ***p-value < 0.001, ****p-value < 0.0001 vs vehicle control group.

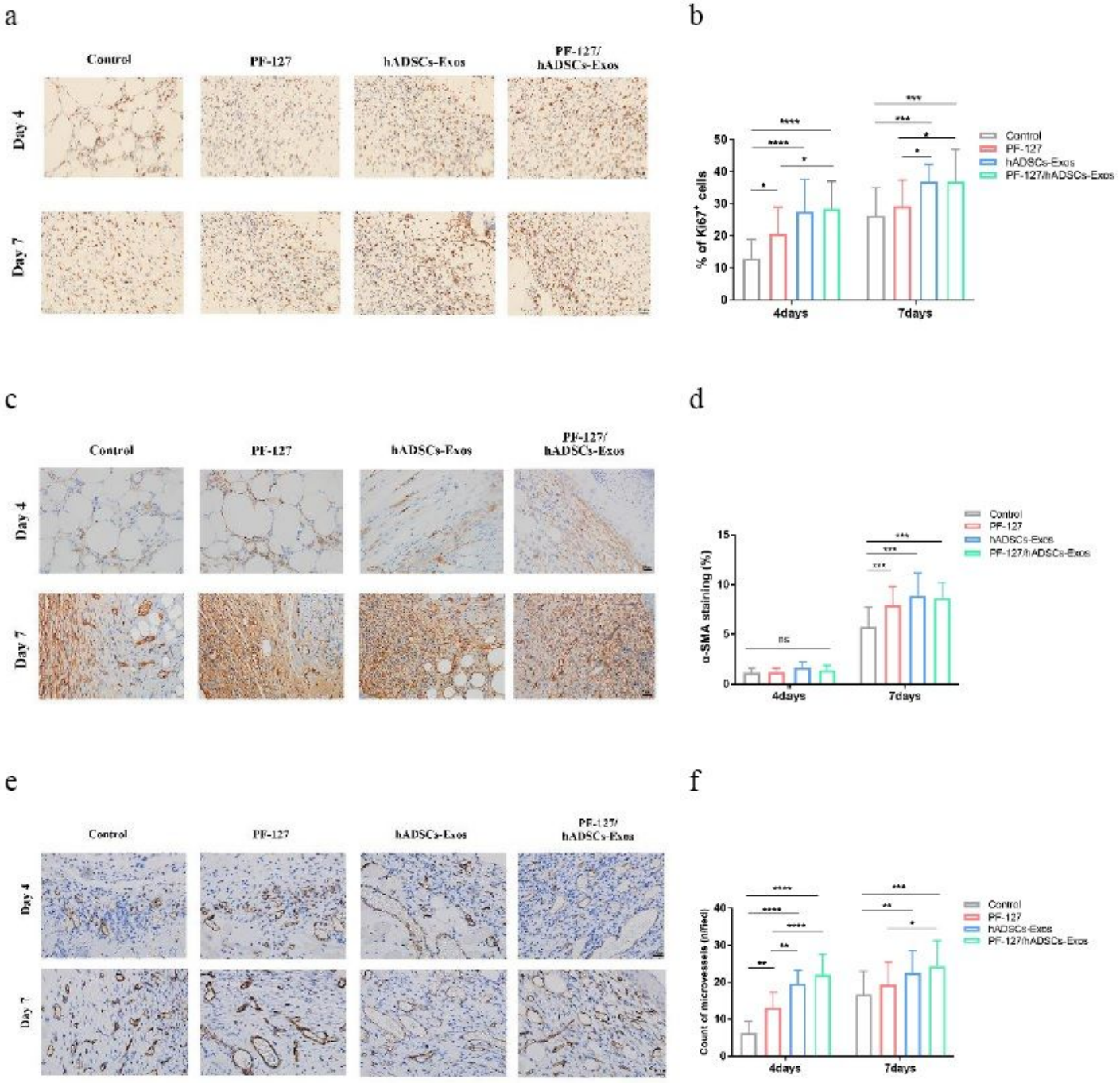

Figure 4

PF-127/hADSCs-Exos improves cell proliferation and angiogenesis. a Images are illustrating Ki67 immunohistochemistry staining on days 4 and 7. Scale bar = 50 μm. b Quantification of the number of Ki67 positive cells in the wound area. c α-SMA staining of myofibroblasts in wound bed at days 4 and 7 post-operative. Scale bar = 50 μm. d Quantification of α-SMA stained tissues. e Representative images of IHC of CD31 on days 4 and 7 wound sections. Scale bar = 50 μm. f Microvessel density analyses of

diverse treatment days 4 and 7 (n = 6). *p-value < 0.05, **p-value < 0.01, ***p-value < 0.001, ****p-value < 0.0001 vs vehicle control group.

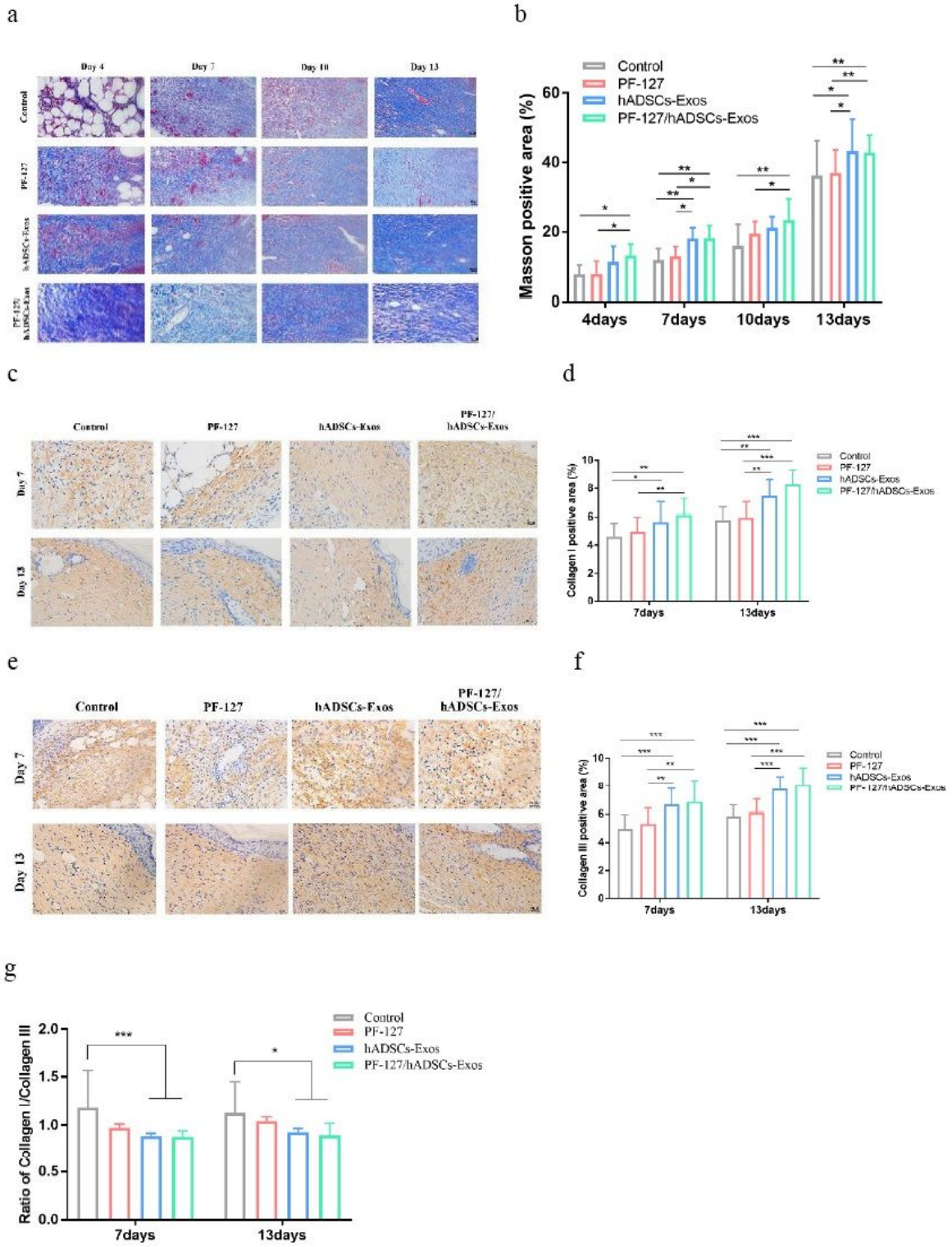

Figure 5

Histochemical analysis of collagen deposition in wounds treated by PF-127/hADSCs-Exos. a Masson staining of collagens deposition in different groups at days 4, 7, 10, and 13 post-wounding. Scale bar = 50 μm. b Quantification of collagens deposition in different groups. c and d Immunohistochemistry

staining images for collagen I and collagen at 7 and 13 days post-wounding, respectively. Scale bar = 50 μm. e Relative density analysis of collagen I and collagen , and the ratio of collagen I/collagen III at 7 and 13 days after surgery, respectively. Results are presented as mean ± standard error of the mean; n = 6 for each group. *p-value < 0.05, **p-value < 0.01, ***p-value < 0.001, ****p-value < 0.0001 vs vehicle control group.

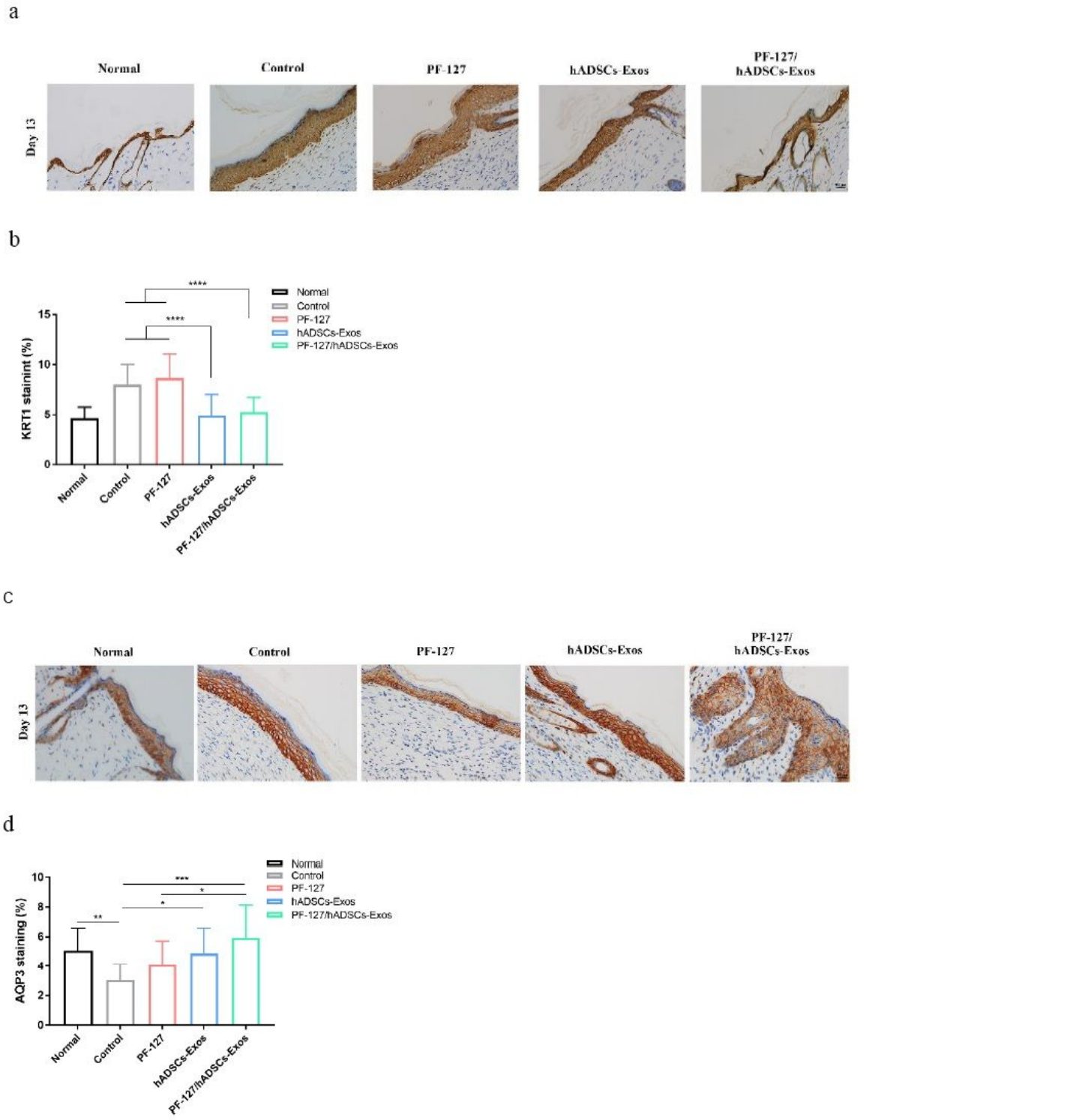

Figure 6

IHC staining of cytokeratin and AQP3 expression in wounds. a IHC images of wound sections stained with cytokeratin (a marker of epithelial cells) at day 13. Scale bar = 50 μm. b Quantification of cytokeratin K1 IHC stained tissues. c IHC images of wound sections stained with AQP3 at day 13. Scale bar = 50 μm. d Quantification of AQP3 IHC stained tissues. Results are presented as mean ± standard error of the mean; n = 6 for each group. *p-value < 0.05, **p-value < 0.01, ***p-value < 0.001 vs vehicle control group.

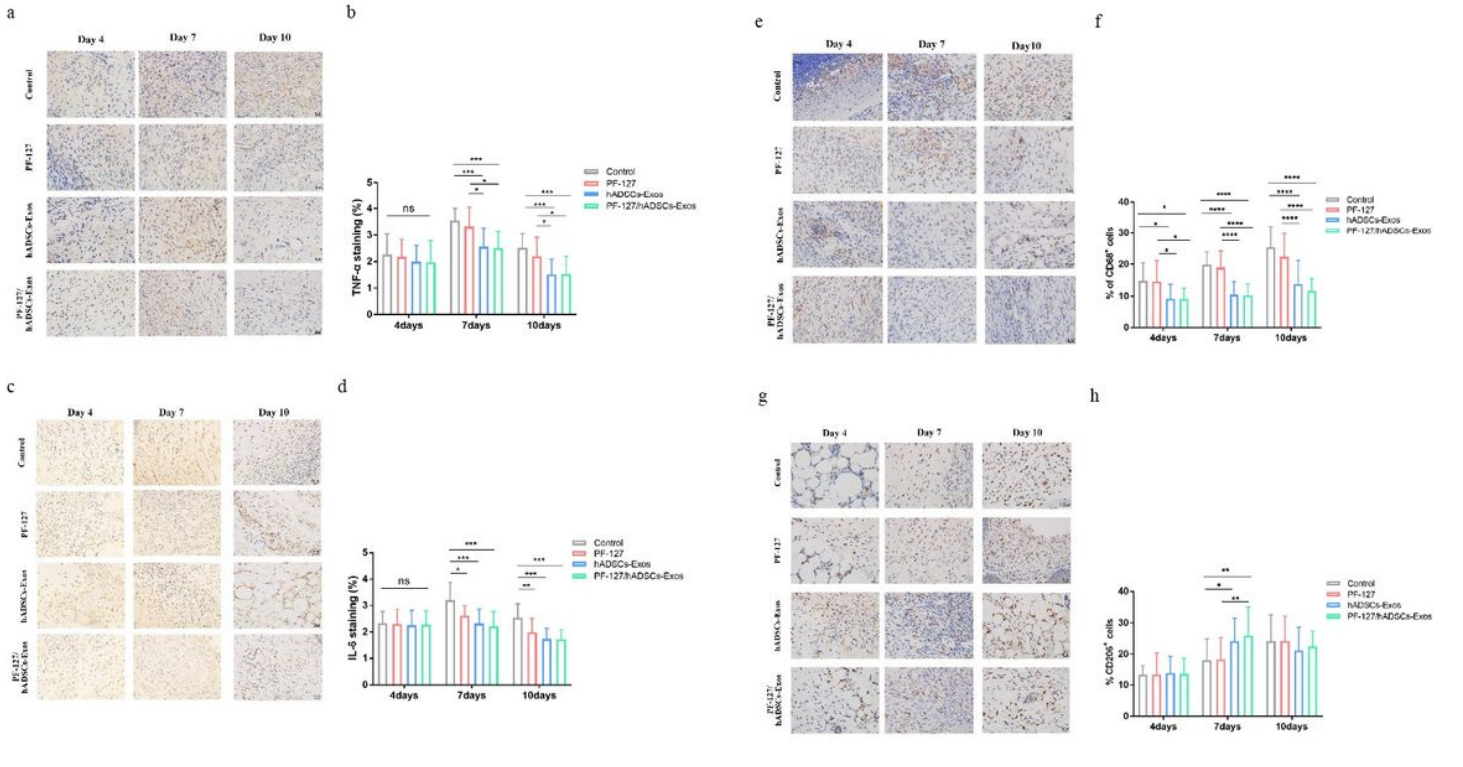

Figure 7

PF-127/hADSCs-Exos complex treatment inhibits inflammatory reaction. a Representative photographs of TNF-α immunostaining at 4, 7, and 10 days after surgery. Scale bar = 50 μm. b Quantification of TNF-α+ IHC stained tissues. c Images illustrating immunohistochemical results of IL-6 at 4, 7, and 10 days after surgery. Scale bar = 50 μm. d Quantification of IL-6+ IHC stained tissues. e IHC images of wound sections stained with CD68 at 4, 7, 10 days post-wounding. Scale bar = 50 μm. f Quantification of the number of CD68 positive cells in the wound area on days 4, 7, and 10. g IHC images of wound sections stained with CD206 at 4, 7, 10 days post-wounding. Scale bar = 50 μm. h Quantification of the number of CD206 positive cells in the wound area on days 4, 7, and 10. Results are presented as mean ± standard error of the mean; n = 6 for each group. * p < 0.05, ** p < 0.01, *** p < 0.001, and **** p < 0.0001 vs vehicle control group.